

PAPER • OPEN ACCESS

## Experimental and Numerical Investigation of Surface Texturing 316L Stainless Steel by Laser Shock Processing

To cite this article: Kangmei Li *et al* 2019 *IOP Conf. Ser.: Earth Environ. Sci.* **252** 022042

View the [article online](#) for updates and enhancements.

# Experimental and Numerical Investigation of Surface Texturing 316L Stainless Steel by Laser Shock Processing

Kangmei Li<sup>1,\*</sup>, Yu Cai<sup>1,a</sup> and Jun Hu<sup>1,b</sup>

<sup>1</sup>College of Mechanical Engineering, Donghua University, 2999 North Renmin Road, Shanghai, 201620, China

\*Corresponding author e-mail: Kangmei Li-lkm718@126.com,

<sup>a</sup>caiyu@mail.dhu.edu.cn, <sup>b</sup>hjmorning@hotmail.com

**Abstract.** Surface texturing is considered as a promising method to reduce friction coefficient and improve wear resistance of frictional pairs. In this study, laser peen texturing (LPT) based on laser shock process is proposed to fabricate dimple array on 316L stainless steel. LPT experiments are carried out to investigate the geometrical characteristics of the micro-dimple. It is shown that LPT is capable of fabricating micro-dimples with good repeatability. Numerical simulation based on finite element method is conducted to further study the process of LPT. It is found that the dimple depth obtained from numerical simulation shows a good agreement with that measured from experiments. Moreover, by means of stress analysis, it is shown that residual compressive stress exists in the specimen, which is supposed to be helpful to improve the tribological performance of frictional pairs.

## 1. Introduction

The wear caused by friction is considered as the main reason for the failure of mechanical systems. At the same time, wear is the major source of energy loss [1]. Therefore, various methods have been developed to reduce friction and wear. One of the most promising solutions is introducing surface textures on friction pairs based on surface texturing technologies. Over the past two decades, the benefits of surface texturing and the effects of texturing parameters on load-carrying capacity were investigated theoretically and experimentally. Parametric studies were carried out in many applications such as bearings [2], engine cylinders [3] and mechanical seals [4]. Friction and wear tests were conducted to investigate the effect of surface textures on tribological performances [5, 6]. It was concluded that surface textures can act as micro-hydrodynamic bearings and help reduce friction and improve load-carrying capacity. Moreover, surface texturing can reserve lubricant and entrap wear debris to improve lubrication conditions.

The ways for generating surface textures include mechanical [7], etching [8] and laser based methods [9]. Mechanical methods are usually contact-type and have loading and unloading processes. Thus tool wear is a prominent problem for these methods, which may affect both the precision and the efficiency of texture fabrication. Although etching methods can generate surface textures accurately and efficiently, no material modification can be induced during these processes.

Laser shock processing (LSP) is a surface treatment method which can improve both mechanical and physical properties of metals. The applications of LSP are mostly focused on surface modification and



macro-scale forming of the metal [10-12]. However, the local plastic deformation induced by laser shock is little concerned. In fact, micro dimples can be fabricated on metal surfaces based on the local plastic deformation effect of LSP. This process is named laser peen texturing (LPT). LPT not only has the advantages of laser surface texturing which based on the thermal effect of laser, but also can avoid the negative effect of material surface integrity induced by the ablation.

Nowadays few studies have been published about the investigation of LPT process and its mechanism is not very clear. In this study, LPT process was adopted to fabricate micro dimples on 316L stainless steel which is widely used in mechanical and biomedical fields. The process mechanism of LPT is preliminarily investigated using experimental and numerical methods.

## 2. LPT experiment

The illustration of LPT is shown in Fig. 1. Laser beam is generated by a Q-switched Nd: YAG laser and then is directed to the sample by reflecting mirrors. A lens is used to focus the laser beam to a required diameter. The sample was fixed on a jig which was mounted on the six-axis robot. The sample is coated with black insulation tapes to avoid the thermal effect caused by laser irradiation. Then flowing water is used as the transparent overlay to confine the expanding plasma against the surface of the target metal, therefore generating a very high pressure. The processing parameters for LPT are listed in Table 1. The samples of 316L stainless steel were cut into square-shape pieces with the dimensions of 50mm×50mm×2mm (length×width×thickness).

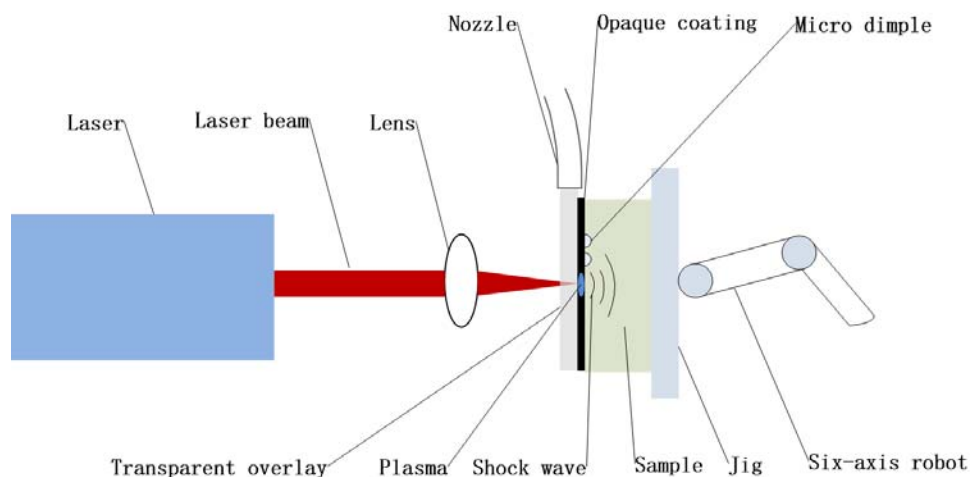


**Figure 1.** Illustration of LPT.

**Table 1.** The processing parameters for LPT.

Parameter	Value
Laser wavelength, $\lambda$ (nm)	1064
FWHM, $\tau$ (ns)	20
Laser frequency, $f$ (Hz)	4
Laser pulse energy, $E$ (J)	0.5, 1, 2, 3
Spot diameter, $D$ (mm)	1.1

## 3. Numerical Simulation of LPT

In order to investigate the process of LPT, numerical simulation of LPT is conducted by using ABAQUS software. For specimen modeling, axisymmetric elements with reduced integration CAX4R are used to model the specimen, while one layer of semi-infinite elements CINAX4 is used to simulate the non-

reflecting boundary condition. The meshed model with the total grid number of 6348 is shown in Fig. 2.

The Johnson-Cook model is used as the material constitutive model to consider the effect of work hardening and strain rate on material flow. Since the thermal effect is negligible for LPT, the Johnson-Cook model is simplified as:

$$\sigma_f = (A + B\bar{\epsilon}^n) \left[ 1 + C \ln \left( \frac{\dot{\epsilon}}{\dot{\epsilon}_0} \right) \right] \quad (1)$$

The material parameters of 316L stainless steel are listed in Table 2.

**Table 2.** Material properties of 316L stainless steel [13].

Density $\rho$ (T/mm <sup>3</sup> )	Young's modulus E (MPa)	Poisson ratio $\mu$	Parameters in Johnson-Cook model			
			A(MPa)	B(MPa)	n	C
7.98e-9	210300	0.30	305	441	0.10	0.057

The typical time history of laser shock pressure during and after laser irradiation is shown in Fig. 3, while the spatial distribution follows the Gaussian spatial distribution:

$$p(r', t) = p(t) \exp\left(-\frac{r'^2}{2R^2}\right) \quad (2)$$

Where  $p$  is the laser shock pressure,  $r'$  is the radial distance from the laser spot center and  $R$  is the radius of the laser spot.

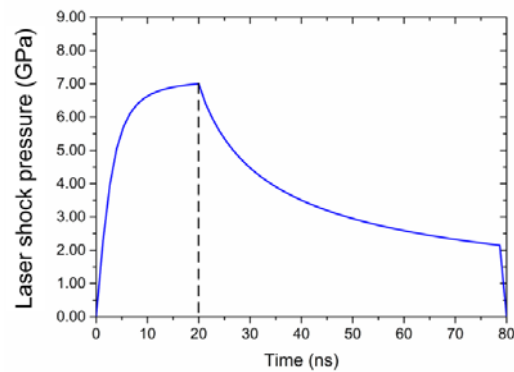
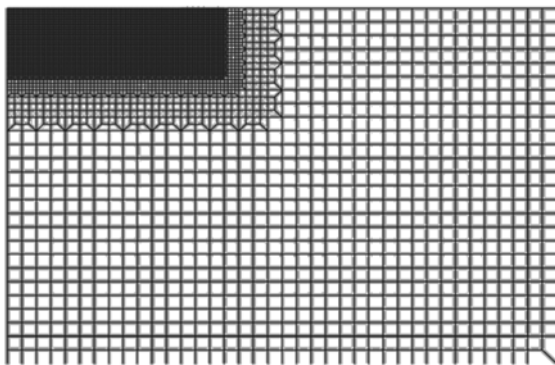


**Figure 2.** The meshed model for LPT simulation. **Figure 3.** The time history of laser shock pressure

In order to make sure the calculation time is long enough to capture the total process of elasto-plastic deformation due to laser shock, the total time for transient analysis in this study is set as 2000ns. After the transient analysis, the spring back analysis is carried out to investigate the material deformation and the stress distribution.

## 4. Results and discussion

### 4.1. Experimental results of LPT

The dimple array fabricated by LPT and the typical 2D profile of micro-dimple are shown in Fig. 4(a) and Fig. 4(b), respectively. It is found that the side-wall of the micro-dimple is tilted instead of vertical and the overall shape is similar to a spherical cap. The probable reason is that the laser spot energy and

the induced shock pressure follow the Gaussian distribution. In addition, slight pile up is observed around the dimple after laser shock process.

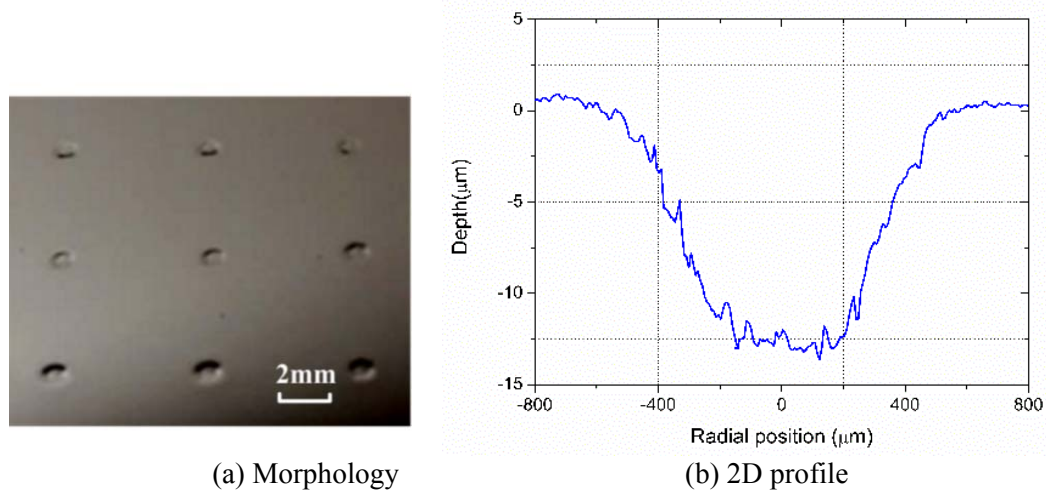
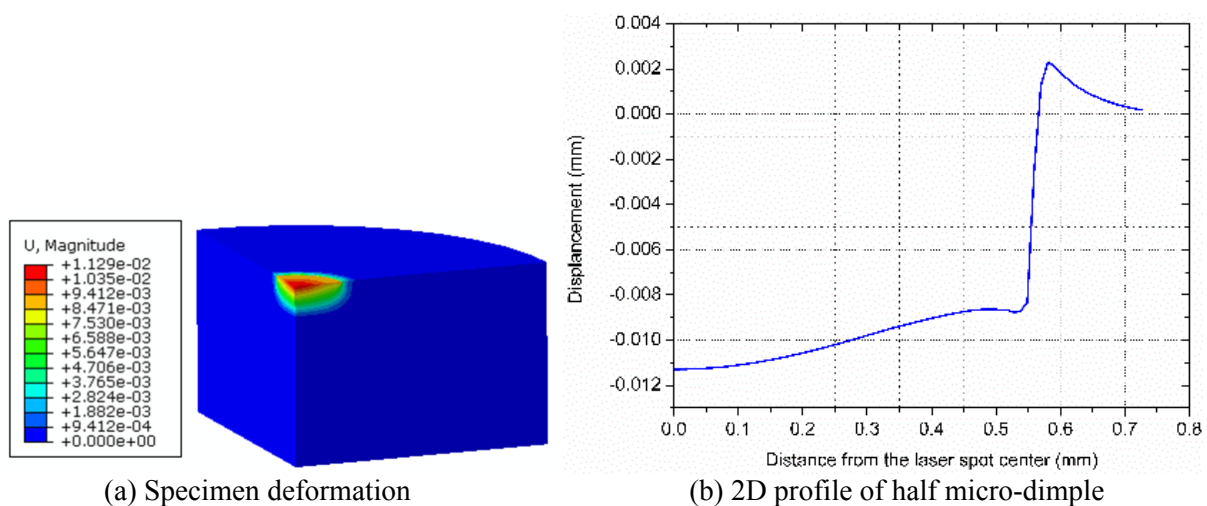


**Figure 4.** Dimple array fabricated on 316L stainless steel by LPT.

#### 4.2. Comparison of deformation obtained from experiment and simulation

In order to analyze the elasto-plastic deformation of the specimen, the typical displacement distribution during the transition process as well as after springback is shown in Fig. 5 and Fig. 6. Fig. 5(a) shows the deformation of the specimen when the laser shock process is finished. It's worth noting that, although the laser shock process stops at about 80ns according to Fig. 3, the deformation of the material continues due to the effect of inertia force (see Fig. 6(a)). In addition, by comparing the 2D profile of half micro-dimple in Fig. 5(b) against that in Fig. 6(b), it is found that the 2D profile after spring back shows deeper dimple depth with more obvious pile up than that when laser shock process stops at about 80ns.



(a) Specimen deformation

(b) 2D profile of half micro-dimple

**Figure 5.** Deformation and displacement at the end of laser shock process ( $t=80$ ns).

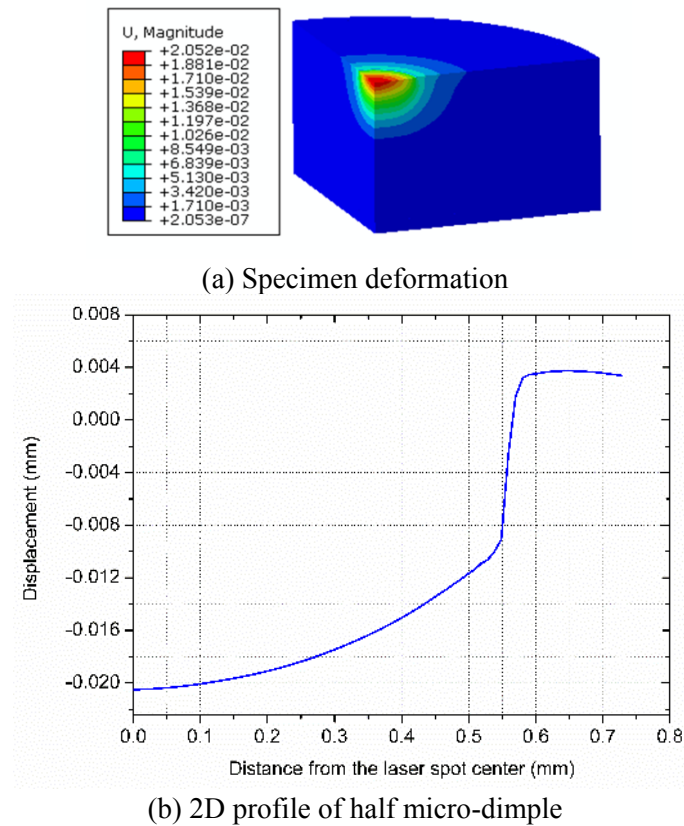


**Figure 6.** Displacement variations in the material at different solving time.

Dimple depth is one of the key parameter to feature the dimple shape. The dimple depths obtained from LPT experiments and numerical simulation are compared (see Fig. 7). It is found that dimple depth increases with laser pulse energy. That is, greater laser pulse energy leads to deeper dimple depth. Moreover, the dimple depths obtained from experiments show a good agreement with that from numerical simulation.

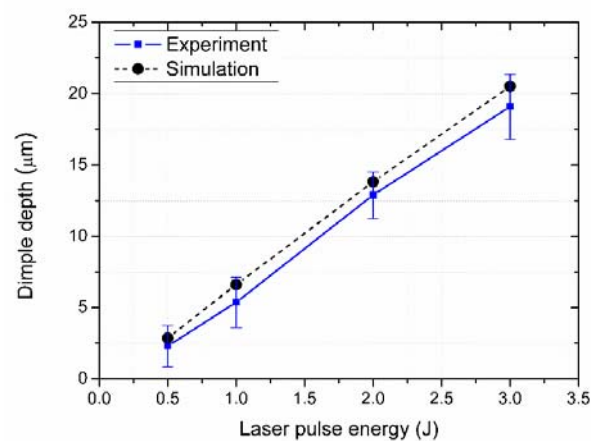
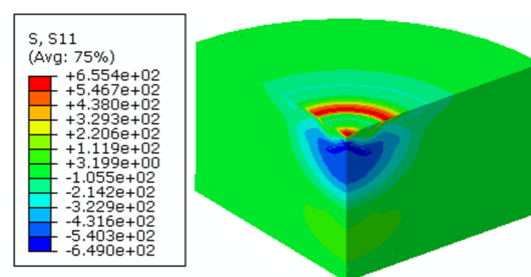


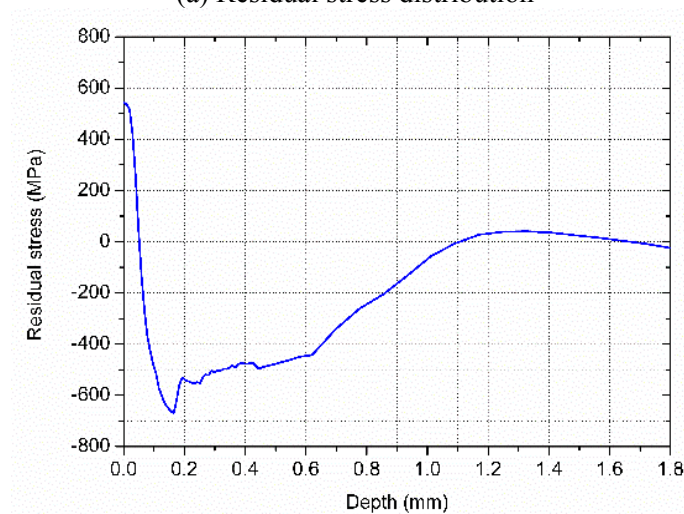
**Figure 7.** Dependence of dimple depth on laser pulse energy.

### 4.3. Stress analysis

Fig. 8 (a) shows the radial stress distribution in the material after spring back. It is found that compressive residual stress exists inside the metallic specimen, which is supposed to be helpful for improving fatigue performance and increasing the service life. Meanwhile, there exist two local residual tensile stress zones which are located at the dimple center and bulge around the dimple, respectively. The residual tensile stress at the center is probably related to the so-called “residual stress whole” phenomenon which is the results of the radial relief wave from the edge of the impact zone and focalizing simultaneously to the center [14]. Fig. 8 (b) shows the residual stress along the symmetry axis. It is found that there exists a residual compressive stress zone beneath the specimen surface, which is helpful for improve the fatigue performance of the specimen.



(a) Residual stress distribution



(b) Residual stress along the symmetry axis

**Figure 8.** Radial stress distribution of the material at different computing time.

## 5. Conclusion

This paper studied the basic mechanism of dimple array on 316L stainless using laser peen texturing. The following conclusions could be drawn:

- (1) By conducting the experiments of laser peen texturing, it is found that laser peen texturing is able to generate dimple array on 316L stainless steel. The overall shape of the micro dimple is like a spherical cap with slight pile up around the dimple.
- (2) The deformation was obtained by both LPT experiments and numerical simulation. It was found that the dimple depths calculated by simulation shows good agreement with those measured in LPT experiments.
- (3) Large residual compressive stress zone was observed beneath the dimple after LPT. The



residual compressive stress zone will be helpful for increasing the fatigue life of friction pairs.

### Acknowledgments

The authors would like to thank the sponsorship from the Fundamental Research Funds for the Central Universities (No. 2232018D3-04, 2232018A3-08), the National Natural Science Foundation of China (Grant No. 51605296) and Shanghai Sailing Program (Grant No. 16YF1408300).

### References

- [1] B. Bhushan, Introduction to tribology, Wiley, New York, U. S. A, 2013.
- [2] I. Etsion, G. Halperin, V. Brizmer and Y. Kligerman, Experimental investigation of laser surface textured parallel thrust bearings, *Tribol. Lett.* 179 (2004) 295-300.
- [3] R. Golloch, G. R. Merker, U. Kessen and S. Brinkmann, Functional properties of microstructured cylinder liner surfaces for internal combustion engines, *Lubr. Sci.* 11 (2005) 307-324.
- [4] I. Etsion, L. Burstein, A model for mechanical seals with regular microsurface structure, *Tribol. Trans.* 39 (1996) 677-683.
- [5] M. J. Baum, L. Heepe, S. N. Gorb, Friction behavior of a microstructured polymer surface inspired by snake skin, *J. Nano.* 5(2014) 83-97.
- [6] M. S. Uddin, T. Ibatan, S. Shankar, Influence of surface texture shape, geometry and orientation on hydrodynamic lubrication performance of plane-to-plane slider surfaces, *Lubr. Sci.* 29(2017) 153-181.
- [7] U. Pettersson, S. Jacobson, Friction and wear properties of micro textured DLC coated surfaces in boundary lubricated sliding, *Tribol. Lett.* 2004 17: 553-559.
- [8] L. S. Stephens, R. Siripuram, M. Hyden, et al. Deterministic micro asperities on bearings and seals using a modified LIGA process, *J. Eng. Gas. Turb. Pow (Trans. ASME)*. 2004 126: 147-154.
- [9] G. Ryk, I. Etsion, Testing piston rings with partial laser surface texturing for friction reduction, *Wear.* 2006 261: 792-796.
- [10] J. Z. Lu, K. Y. Luo, F. Z. Dai, et al. Effects of multiple laser shock processing (LSP) impacts on mechanical properties and wear behaviors of AISI 8620 steel, *Mater. Sci. Eng A.* 2012 536: 57-63.
- [11] C. Rubio-Gonza'lez, C. Felix-Martinez, G. Gomez-Rosas, et al. Effect of laser shock processing on fatigue crack growth of duplex stainless steel, *Mater. Sci. Eng. A.* 2011 528: 914-919.
- [12] C. Ye, G. J. Cheng, Laser shock peening of nanoparticles integrated alloys: numerical simulation and experiments, *J. Manu. Sci. Eng.* 132 (2010) 0610171-1-7.
- [13] H. Chandrasekaran, R. M'saoubi, H. Chazal, Modelling of material flow stress in chip formation process from orthogonal milling and split Hopkinson bar tests, *J. Mach. Sci. Tech.* 2005 9(1): 131-145.
- [14] Y. Hu, Z. Yao, Numerical simulation and experimentation of overlapping laser shock processing with symmetry cell, *Mach. Tool. Manu.* 48(2008) 152-162.